Aodhan Sweeney[1], Qiang Fu[1,2], Hamid A. Pahlavan[1,3], Peter Haynes[2]

[1]University of Washington, Department of Atmospheric Sciences

[2]University of Cambridge, Department of Applied Mathematics and Theoretical Physics

[3]Rice University, Department of Mechanical Engineering

Corresponding author: Aodhan Sweeney (`aodhan@uw.edu`)

Key Points:

- The Quasi-Biennial Oscillation (QBO) significantly impacts high equatorial clouds during boreal spring and early summer

- QBO-related cloud changes result in a statistically significant change in the longwave cloud radiative effect by ~1Wm^{-2}

- The seasonality of the QBO impact on clouds is synchronized with upper tropospheric intrusions of QBO related temperature and zonal wind

Abstract

The Quasi-Biennial Oscillation (QBO) dominates the interannual variability in the tropical lower stratosphere and is characterized by the descent of alternating easterly and westerly zonal winds. The QBO impact on tropical clouds and convection has received great attention in recent years due to its implications for weather and climate. In this study, a 15-year record of high vertical resolution observations from CALIPSO are used to document the QBO impact on equatorial (10°S-10°N) clouds. Observations from radio occultations, the CERES instrument, and the ERA5 reanalysis are also used to document the QBO impact on temperature, radiative energy budget, and zonal wind. It is shown that the QBO impact on zonal mean equatorial cloud fraction has a strong seasonality. The strongest cloud fraction response to the QBO occurs in boreal spring and early summer extending down to ~12 km and results in a significant longwave cloud radiative effect anomaly. The seasonality of the cloud fraction changes is synchronized with those of temperature and zonal wind in the tropical upper troposphere.

Plain Language Summary

Approximately every two years, eastward or westward winds in the stratosphere above the equator reverse their direction. This pattern of alternating wind direction is called the Quasi-Biennial Oscillation (QBO). It has been suggested that the QBO might affect the tropical troposphere including month-to-month variability of precipitation patterns, and the frequency or strength of tropical cyclones. However, the robustness of these impacts and the associated physical mechanism are still under debate. Of particular interest is the QBO impact on clouds which can be a signal of storminess and can impact weather and climate. In this study, we use fine vertical resolution satellite data to examine the QBO-cloud connections. We find that the QBO impact on equatorial clouds spans a

deep vertical extent of the upper troposphere and shows a strong seasonality. These cloud responses imply a significant change in the Earth's radiation budget. We also find that the seasonal variations in cloud responses are concurrent with seasonal variation in QBO-related wind speed and temperature signals. These changes are most significant during northern hemisphere spring and early summer.

1 Introduction

The Quasi-Biennial Oscillation (QBO) is the main mode of variability in the tropical lower stratosphere and is characterized by descending regions of alternating zonal winds and temperature anomalies connected through thermal wind balance (Lindzen and Holton, 1968; Holton and Lindzen, 1972; Plumb and Bell, 1982; Andrews et al., 1987, Baldwin et al., 2001; Fueglistaler and Haynes, 2005; Pahlavan et al., 2021a). Although the QBO zonal wind amplitude decreases rapidly below 50 hPa (e.g., Saravanan, 1990; Match and Fueglistaler, 2019) the QBO has been shown to impact the troposphere. One important route of QBO influence on the extratropical troposphere is through the QBO modulation of the stratospheric polar vortex (Holton and Tan, 1980; Holton and Tan, 1982; Baldwin et al., 2001; Anstey and Shepherd, 2014; Lu et al., 2020). Another potentially more direct impact is on the tropical troposphere through the QBO modulation of tropical clouds and convection (Collimore et al., 2003; Liess and Geller, 2012; Son et al., 2017; Tseng and Fu, 2017a; Haynes et al., 2021; Hitchman et al., 2021). It has been suggested that the direct impact of the QBO on tropical clouds and convection may work by modulating the thermodynamic (temperature and static stability) and dynamic (vertical wind shear) properties of the transition layer between the tropical troposphere and stratosphere (Giorgetta et al., 1999; Collimore et al., 2003; Gray et al., 2018; Tseng and Fu, 2017a; Martin et al., 2019; Haynes et al., 2021). This layer is called the tropical tropopause layer (TTL) and extends from ~14.5 to 18.5 km (Fu et al., 2007; Fueglistalaer et al., 2009).

Interest in the QBO direct impact on the tropical troposphere has recently been invigorated due to the correlation between the Madden-Julian Oscillation (MJO) and the QBO (Yoo and Son, 2016; Son et al., 2017; Zhang and Zhang, 2018; Martin et al., 2021b; Lin and Emanuel, 2022). Many attempts to explain the connection focus on the anomalously cold TTL temperatures, decreased TTL static stability, and increased TTL cirrus clouds when the QBO is easterly near 50 hPa (e.g., Son et al., 2017; Hendon and Abhik, 2018; Klotzbach et al., 2019; Densmore et al., 2019; Sakaeda et al., 2020). Curiously, the QBO-MJO connection has been shown to be only present in boreal winter (e.g., Yoo and Son, 2016), while QBO impacts on tropical convection more broadly have also been found during other seasons (Giorgetta et al., 1999; Collimore et al., 2003; Gray et al., 2018; Densmore et al., 2019). Studies also show that the QBO impact on the thermodynamic and dynamic properties of the TTL varies strongly across seasons (Sakaeda et al., 2020; Tegtmeier et al., 2020; Hitchman et al., 2021; Martin et al., 2021a). To explain these variations, these studies have tended to

focus on the seasonal variation in the troposphere without regard to potential systematic seasonal variation in the QBO above the tropopause (Son et al., 2017; Tegtmeier et al., 2020). In fact, it has been shown that the QBO itself undergoes strong seasonality, showing seasonal variations in the QBO acceleration near 50 and 70 hPa (Dunkerton, 1990; Coy et al., 2020). This may be cause by the seasonality of the QBO wave forcing at these levels (Maruyama, 1991; Tindall et al., 2006; Sjoberg et al., 2017) or by the Brewer-Dobson Circulation (BDC) which potentially affects QBO descent rate throughout much of the stratosphere (Kinnersley and Pawson, 1996; Hampson and Haynes, 2004; Rajendran et al., 2018; Coy et al., 2020). Whether these seasonal variations are important for the direct impact of the QBO on the tropical troposphere is still not well known.

Previous investigations of the QBO direct impact on the tropical troposphere showed anomalies in temperature, zonal wind, clouds, deep convection, and even Outgoing Longwave Radiation (OLR) (e.g., Huesmann and Hitchman, 2001; Collimore et al., 2003). Interpretations of these results were limited by the poor vertical resolution of reanalysis, strong zonal and seasonal variations, and inconsistent QBO definitions. More recent work using improved reanalysis products and precipitation data has confirmed the strong longitudinal and seasonal variation in the tropical tropospheric signal (e.g., Liess and Geller, 2012; Gray et al., 2018). This variation complicates analysis of the QBO direct impact and the physical mechanisms responsible.

An important component of the QBO direct impact maybe its effect on high altitude cirrus clouds which can heat the troposphere but cool the stratosphere (Fu et al., 2018; Fueglistaler and Fu, 2006), decreasing the stability of the TTL. These clouds have also been implicated as a potentially important modulator of the QBO-MJO connection (e.g., Son et al., 2017; Martin et al., 2021b; Lin and Emanuel, 2022). Apart from these potential couplings, high altitude cirrus clouds are also important because of their impact on the TTL radiative heating rate, troposphere-stratosphere transport, and TTL thermal structure (Hartmann et al., 2001; Corti et al., 2005; Corti et al., 2006; Yang et al., 2010; Flury et al., 2012; Davis et al., 2013; Dessler et al., 2013; Hong et al., 2016; Tseng and Fu, 2017a; Fu et al., 2018; Wang and Fu, 2021). These cirrus clouds also exhibit a greenhouse effect, thus impacting the cloud radiative effect (CRE) which can change the energy budget of the tropics.

Accurate documentation of the QBO direct impact requires high vertical resolution observations in the TTL, where communication between the tropical stratosphere and troposphere takes place. This study documents the seasonality of the QBO vertical impact on equatorial high clouds using high vertical resolution CALIPSO lidar data. Temperature and radiative energy budget observations are obtained independently from GPSRO-and CERES instruments. The QBO response in zonal wind is analyzed using ERA5 reanalysis data. This study focuses primarily on the zonal mean QBO impact in order to simplify complications due to zonal asymmetries. Unique to this study is the documentation of the QBO impact on vertical profiles of clouds and temperature as it

3

descends from the lower stratosphere into the TTL for various seasons. We find that the QBO impact on clouds undergoes large seasonal variations reaching its maximum depth in boreal spring and early summer three months after the QBO-related zonal wind has maximized at the 50 hPa level. These deep cloud fraction anomalies extend from above the tropopause to as low as ~12 km (~180 hPa). These cloud fraction anomalies are concurrent with a statistically significant QBO impact on the equatorial longwave CRE. QBO-induced changes in cloud fraction and the CRE are synchronized with changes in temperature, vertical temperature gradient, and zonal wind in the TTL. Section two describes information about the data and methods used in this study, section three shows the results, and section four provides the potential causes and implications of these results.

2 Data and Methods

2.1 Satellite observations and ERA5 reanalysis

a. CALIPSO cloud observations

The CALIPSO satellite was launched in April 2006 into a sun synchronous orbit with local equatorial crossing times at 01:30 and 13:30 (Winker et al., 2010). The main instrument used in this study is the Cloud-Aerosol Lidar with Orthogonal Polarization (CALIOP) dual wavelength polarization sensitive lidar. CALIOP can provide information of cloud layers with optical depth from ~0.01 to ~4 at which the CALIOP signal becomes fully attenuated. In this study we use the Level 2 V4.2 5-km Merged Layer Product with a vertical resolution of 60 m from June of 2006 to December of 2020. The primary quantity used from the CALIPSO data is the cloud fraction above 11 km, which is defined as the number of detections of clouds divided by the total number of observations in each 2.5°x2.5° grid cell.

Previous versions of the CALIOP data did not identify clouds above the lapse rate tropopause, potentially missing a large amount of TTL cirrus clouds (Tseng and Fu, 2017b). The recent V4 release of CALIOP data has improved detection of TTL cirrus by applying the cloud-aerosol distinction algorithm to layers above the lapse-rate tropopause. With these V4 changes, we find significant amounts of stratospheric aerosols that are misidentified as TTL cirrus clouds. These stratospheric aerosols appear to be directly linked to tropical volcanic eruptions (Tseng and Fu, 2017b). Tseng and Fu (2017b) found that previous versions of the Level 2 data could be used to accurately identify TTL cirrus clouds above the lapse rate tropopause by using the volume depolarization ratio (VDR). We similarly apply this VDR threshold of VDR > 0.12 for all layers identified above the lapse-rate tropopause. This largely eliminates the amount of falsely identified TTL cirrus clouds in February-April of 2014, which corresponds to the 2014 Kelud eruption in Indonesia.

b. Global positioning system-radio occultation temperature observations

Temperature profile data comes from Global Positioning System-Radio Occul-

tation (GPS-RO) receivers onboard the COSMIC-1, MetOp-A and MetOp-B satellites which are archived at the University Corporation for Atmospheric Research (UCAR) (Sweeney and Fu, 2021). We use GPS-RO data from June of 2006 to December of 2020. Radio occultations are retrieved using an active limb sounding technique, allowing for retrieval of bending angle and refractivity, which can be used to derive temperature (Kursinski et al., 1997). GPS-RO temperature profiles have low error (less than 0.1 K), as well as high vertical resolution (0.5 km) in the tropical upper troposphere, and lower stratosphere but relatively coarse horizontal resolution (about 200 km) (Kursinski et al., 1997; Kuo et al., 2004; Zeng et al., 2019). We use the level-2 wetPrf product (Sweeney and Fu, 2021), which provides estimates of temperature including the effects of moisture and is equivalent to the dry profiles when humidity is negligible (as it is in the TTL) (Kursinski et al., 1997).

c. CERES observations and ERA5 reanalysis

To quantify the QBO impact on the CRE at the top of the atmosphere, we use the level three CERES Energy Balance and Filled Climate Data Record (Loeb et al., 2018). Data used from this record spans 2006-2020 and is provided at 1°x1° horizontal resolution. The ERA5 reanalysis is used to create the QBO index, analyze the QBO impacts on zonal wind, and diagnose the zonal wind tendencies. The QBO index and analysis of QBO zonal winds is done using monthly mean ERA5 data with 1°x1° horizontal resolution. The zonal wind tendency analysis is completed using 1°x1° horizontal resolution with 6-hourly temporal resolution.

2.2 QBO index and analysis method

The QBO index is the 10°S-10°N 50 hPa zonal mean zonal wind anomalies taken from the ERA5 reanalysis (Pahlavan et al., 2021a; Martin et al., 2021a). As is well-known, the phase of the QBO varies strongly with height. Correlations of QBO winds with other variables will therefore depend strongly on the height at which the wind is measured. One approach has been to use an EOF representation of the QBO (Wallace et al., 1993), however this has the disadvantage that the phase is determined by combining information from many levels, which may not be optimal when considering variations in the lower stratosphere. The approach here is to use 50 hPa winds, but to consider different lagged correlation with these winds (e.g., Liess and Geller, 2012; Tseng and Fu, 2017a; Ding and Fu, 2018). The 50 hPa (~21 km) level sits above the TTL. Assuming the QBO descent rate is ~1km/month, then using the QBO index at 50 hPa with leads from zero to four months will allow for assessment of the QBO impact as it descends into the TTL.

Satellite observations and the ERA5 reanalysis data are used to document the impact of the QBO on equatorial cloud fraction, temperature, zonal wind, and radiative energy budget. To focus on the interannual variability caused by the QBO, the seasonal cycle is first removed from all variables. Anomalies to the seasonal cycle are denoted in figures and throughout the text using the notation

5

X' where X is a given variable of interest and ' denotes the anomaly after removing the seasonal cycle. This study isolates the QBO impact by averaging months of data where the 50 hPa zonal wind is above and below 0.5 standard deviations from the mean corresponding to westerly (QBOW) and easterly (QBOE) phases respectively (e.g., Yoo and Son, 2016; Son et al., 2017; Martin et al., 2021a). Note that "impact" throughout the text refers to the QBO signal in each variable X after constructing the QBOW-QBOE composite and is not necessarily meant to imply causality. To reduce the effect of month-to-month variability, we analyze the seasonality of the QBO impact using composites created using three consecutive months instead of each month individually. Significance of the difference composites between QBOW and QBOE is tested using a bootstrap method. For each iteration of the bootstrap a QBOW and QBOE composite as well as a difference composite can be found. The difference composites can then be used to create a distribution from which a standard deviation can be calculated. The QBO impact is deemed statistically significant if the observed QBOW-QBOE difference of that value is greater than two standard deviations away from zero. The analysis was repeated using the regression approach and statistical significance was retested accounting for autocorrelation leading to similar results (not shown).

3 Results

3.1 Zonal Mean Cloud Fraction

Figure 1 shows the impact of the QBO on equatorial cloud fraction using the QBOW-QBOE cloud fraction composites. Each panel represents cloud fraction response as a function of season and height from ~11 to 20 km. Columns represent months of lead used for the QBO index, and rows show the partitioning of different cloud types. The first row shows the QBO response in cloud fraction considering all clouds, called All Cloud fraction. The All Cloud fractions are further divided into three subtypes. The TTL Cirrus (row two in Fig. 1) are clouds with bases above 14.5 km (Tseng and Fu, 2017a). The Opaque Clouds (row four in Fig.1) are the cloud layers where the lidar signal becomes saturated, which are often associated with deep convection and thick anvil. Because the Opaque Clouds saturate the lidar no clouds below are detectible. We thus assume that all layers below the top of the opaque cloud are also cloudy layers. Other Cirrus (row three in Fig. 1) are clouds that are not TTL Cirrus or Opaque Clouds, which are associated with thin anvil and cirrus clouds that have bases below 14.5 km (Sokol and Hartmann, 2020). In all plots, the thick black line represents the mean tropopause height from the GPS-RO data, and the stippling indicates regions where results are significant at 2σ.
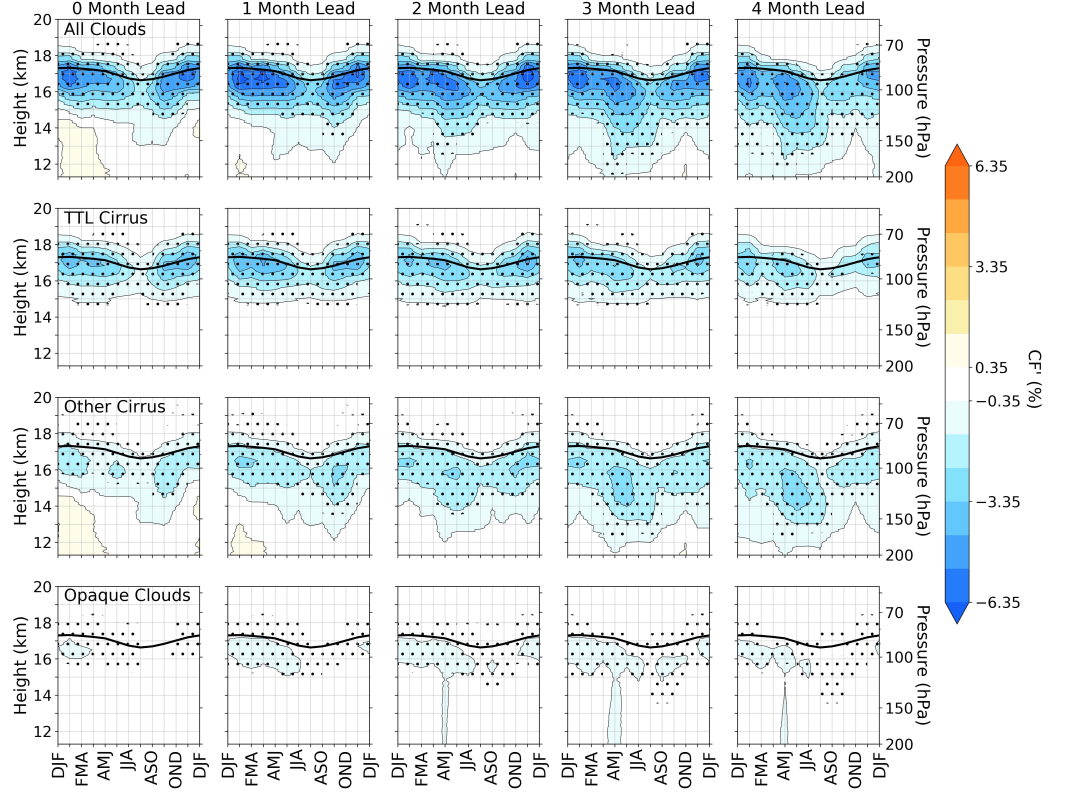
Figure 1: Seasonality of zonal-mean QBOW-QBOE anomaly composites averaged over 10°S-10°N as a function of height for All Cloud fractions (row one), which are further divided into TTL Cirrus (row two), Other Cirrus (row three), and Opaque Clouds (row four). The columns represent various leads of the QBO index used. Thick black lines show the mean tropopause. Stippling indicates regions where impact is significant at a 2σ confidence interval.

All significant cloud fraction changes are negative. This is consistent with the idea that the warmer temperatures associated with QBOW decrease cloud fraction, whereas the opposite is true for QBOE. All Cloud fraction changes (row 1 of Fig. 1) maximize below the tropopause, and a large seasonality in magnitude is evident regardless of lead time chosen. The largest All Cloud fraction impacts occur below the tropopause level using a one-month lead of the QBO index from JFM-MJJ and from SON-NDJ, reaching a maximum magnitude of up to 8%. The weakest response at this level is in JAS and may be caused by

the weak QBO-related temperature anomalies (Sakaeda et al., 2020; Hitchman et al., 2021; Martin et al., 2021a) and small climatological cloud amount (Tseng and Fu, 2017b) during these months. A much weaker local minimum also occurs in DJF.

In addition to the magnitude of the cloud fraction responses, the vertical extent (i.e., thickness of the cloud fraction change) is also sensitive to lead time and season. The vertical extent of the statistically significant region using a zero-month lead is roughly constant across seasons, with minima in JAS and DJF. Using a two-month lead, a vertically extensive maximum near MAM-AMJ becomes more apparent, and statistically significant changes at this time are observed below 14 km. Using a three-month lead, significant cloud fraction responses are observed as low as 12 km. These deep cloud fraction changes are only associated with the boreal spring and early summer. This deep cloud fraction change in boreal spring and summer can be reproduced using QBO indices defined at the 30 or 70 hPa levels, but with the maximum impact occurring at different lead times (see supplementary Figures S1 and S2). These results were also recreated after linearly regressing out the ENSO 3.4 signal with no noticeable changes, suggesting that the ENSO has little impact on the zonal mean high clouds (Tseng and Fu, 2017a).

Partitioning All Cloud fraction into its constituent groups reveals that the largest contributor to the changes in All Cloud fraction in the TTL are TTL Cirrus (row two in Fig. 1). Many studies have shown that the QBO can impact the interannual variability of TTL Cirrus (e.g., Flury et al., 2012; Davis et al., 2013; Tseng and Fu, 2017a). The TTL Cirrus response reaches its maximum of ~4.5% in JFM-MAM when using a one-month lead of the QBO index. TTL Cirrus changes also undergo strong seasonality in their magnitude and vertical extent. The minimum vertical extent is observed in JAS, and a much weaker secondary minimum is observed in DJF which is most evident at lead times of two and less months. In the TTL, QBO related changes in the Other Cirrus (row three in Fig. 1) are weaker than changes seen in the TTL Cirrus but much more vertically extensive because they do not have the same 14.5 km cloud base threshold. Other Cirrus changes extend from above the tropopause to below the TTL, which is largely responsible for the significant deep intrusion of All Cloud fraction changes at a three-month lead during boreal spring and summer. The fourth row of Fig. 1 shows changes in Opaque Clouds. Zonal mean Opaque Cloud responses are weak but are still more apparent from JFM to MJJ and ASO when using QBO leads of between one and three months. Fig. 1 shows that the QBO impact on zonal mean equatorial cloud fraction is sensitive to both the season and lead time chosen. Additionally, TTL Cirrus clouds and Other Cirrus clouds have a different seasonality of QBO response. The high magnitude and vertically extensive changes in cloud fraction raise questions on whether these cloud changes lead to significant changes in the radiative energy budget.

Figure 2 shows the longwave cloud radiative effect (CRE) as a function of lead

time and season. The longwave CRE is derived from the independent CERES observations. The red (blue) line in Fig. 2 shows the composite longwave CRE' for QBOW (QBOE) and the black line shows QBOW-QBOE. Gray shading around the QBOW-QBOE composite shows the 2σ confidence interval. Cirrus clouds have a greenhouse effect and thus a positive longwave CRE. Decreases in high cloud fraction observed in Fig. 1 should be associated with decreases in the longwave CRE (see black line in Fig. 2). Consistent with this idea, the QBOE in Fig. 2 (blue line) generally shows increases in the CRE'. But the QBOW (red line) shows little to no CRE' changes, suggesting that the QBOW may not impact clouds as much as the QBOE (Liess and Geller, 2012). Although observed changes in the CRE' (black line in Fig. 2) are largely consistent with observed changes in cloud fraction (Fig. 1), the only statistically significant CRE response to QBO is observed during boreal spring and summer when using QBO leads of three and four months. This change in longwave CRE is synchronized with the deep changes in cloud fraction observed in Fig. 1. This result lays out a potential connection between the QBO and the radiative energy budget through the impact on clouds. The perturbed cloud presence leads to a statistically significant decrease in the longwave CRE of ~1 W/m^2.

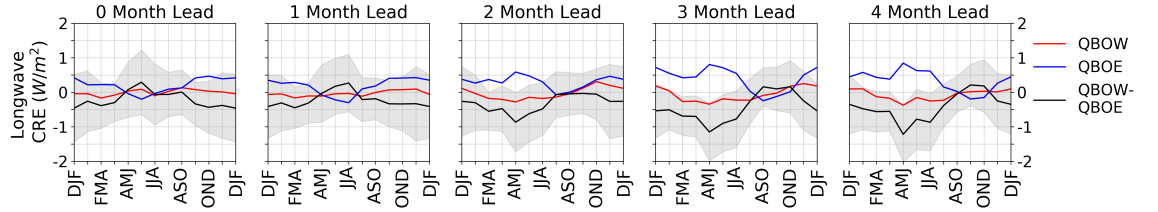Figure 2: Seasonality of the QBO impact on longwave cloud radiative effect averaged over 10°S-10°N. The black line is the QBOW (red line) composite minus the QBOE (blue line) composite. The columns represent various leads of the QBO index. The shaded region shows the 2σ confidence intervals.

Previous studies have suggested large zonal variations of the QBO impact on the TTL (Collimore et al., 2003; Son et al., 2017; Tegtmeier et al., 2020). Figure 3 provides the zonal structure of cloud fraction response to the QBO averaged over 10°S-10°N. For brevity, we only show QBOW-QBOE composites for a three-month QBO lead in DJF, AMJ, and JAS seasons. The ENSO 3.4 signal was first regressed out before deriving the QBO composites. Continental outlines from 10°S-10°N are provided at the bottom of each column. DJF, AMJ, and JAS are selected because of the previously suggested QBO-MJO connection season (DJF), and maximum (AMJ) and minimum (JAS) zonal all cloud fraction response seasons (Fig. 1). A climatology of zonal cloud fraction for these three seasons is provided in the Figure S3. Taking zonal averages of the fields in Fig. 3 corresponds with the relevant month ranges in the three-month lead column of Fig. 1. All cloud fraction changes in both DJF and AMJ reach amplitudes of ~10% but have different zonal structures leading to larger zonal mean cloud fraction anomalies in AMJ. Negative changes over the Indian Ocean and those

over the eastern Pacific in AMJ enforce each other, while during DJF the positive changes over the eastern Pacific partly cancel the negative ones over the western Pacific. The east-west contrast in the QBO signal in DJF is consistent with QBO-associated changes in the Walker circulation in boreal winter, which is associated with a relative reduction in precipitation in the western Pacific and increase in the easter Pacific during QBOW compared to QBOE (Liess and Geller, 2012; Yamazaki et al., 2020).
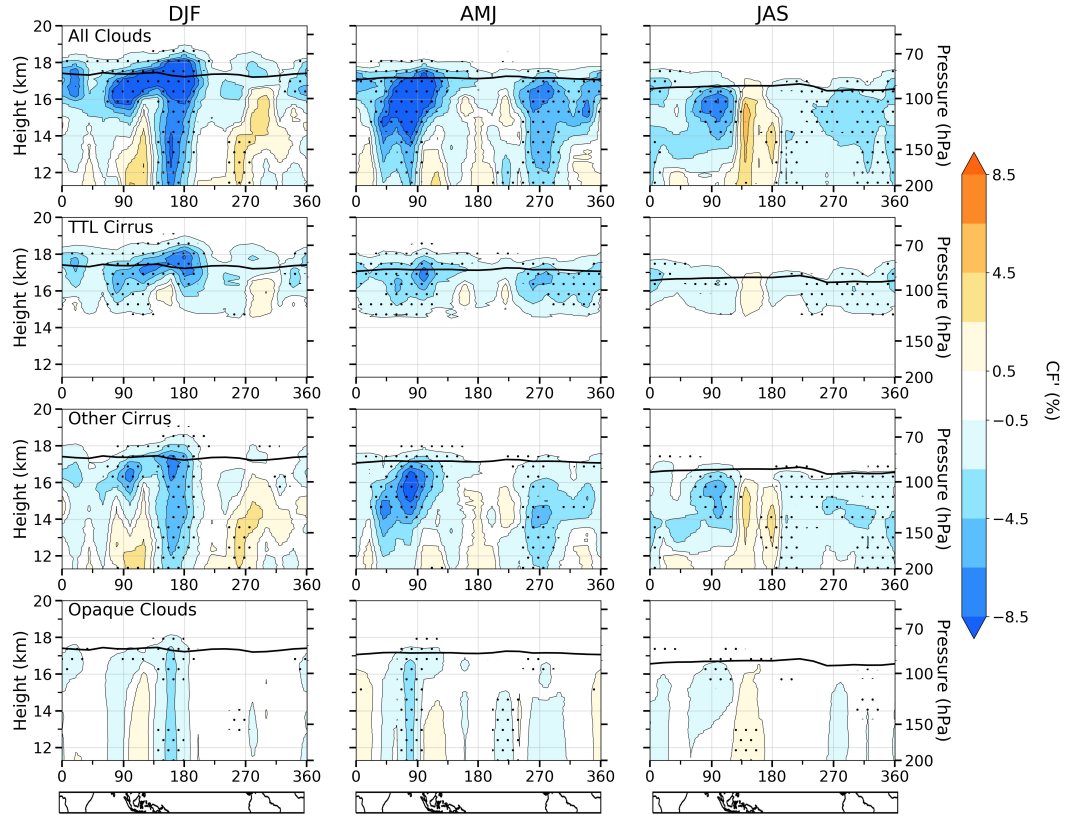

Figure 3: Zonal distribution of QBOW-QBOE anomaly composites averaged over 10°S-10°N as a function of height for All Cloud fractions (row one), TTL Cirrus (row two), Other Cirrus (row three), and Opaque Clouds (row four), in DJF (column 1), AMJ (column 2), and JAS (column 3) seasons. The QBO lead is three months. Thick black lines show the tropopause. Stippling regions indicate that anomaly is significant at a 2σ confidence interval. Continental outlines of the 10°S-10°N region are provided below each column.

In the TTL, all cloud fraction in DJF shows a strong reduction that is eastward tilting with height and extends from the Indian Ocean to the western Pacific. These features are also present during DJF in the TTL Cirrus and Other Cirrus anomalies. The vertically eastward tilting portion of the cirrus structure is reminiscent of the vertically propagating Kelvin wave driven by tropical convection (Virts et al., 2010; Virts and Wallace, 2014; Hendon and Abhik, 2018). This feature can be considered as the QBO modulation of cirrus clouds associated with Kelvin waves in the TTL. TTL Cirrus fraction anomalies in AMJ show a weaker cirrus deck tilt, but All Cloud fraction responses over the MJO active regions over the Indian Ocean have the same sign all the way down due to the vertically extensive signature of both Other Cirrus and Opaque Clouds. The largest Opaque Cloud anomalies are found in DJF over the western Pacific and in AMJ over the Indian Ocean, consistent with the regions of deep intrusions of Other Cirrus cloud fraction response. Opposite to results of DJF, significant positive Opaque Cloud responses are found over the western Pacific in JAS (Collimore et al., 2003; Gray et al., 2018).

The height-longitude structure of the QBO response in clouds shown in Fig. 3 may be compared with the corresponding structure of the climatological cloud fraction fields shown in Fig. S3. Not surprisingly, the larger magnitude anomalies tend to be associated with the regions where cloud fraction is larger in the climatology. Maximum QBO-related cloud responses are typically above the climatological cloud maxima. Longitudinal variations of the cloud response are typically on the eastern and western flanks of climatological maxima in DJF and AMJ, respectively. Thus, in some cases, the QBOW-QBOE changes can be interpreted as a longitudinal shift in the cloudiness. However, the direction of this shift is not always the same and is sometimes eastward (e.g., DJF in the western Pacific) and sometimes westward (e.g., AMJ in the Indian Ocean). More straightforward is the reduction in cloud fraction in the TTL for the QBOW-QBOE composite.

3.2 Temperature and Zonal Wind in the TTL

Previous studies have shown that the variability of tropical high cloud fraction, especially that of TTL cirrus clouds, is frequently linked to changes in temperature and vertical temperature gradient (Kim et al., 2016; Tseng and Fu, 2017a; Chang and L'Ecuyer, 2020). The QBO may thus contribute to the interannual variability of these clouds by changing the thermodynamic properties of the TTL (Flury et al., 2012; Davis et al., 2013; Tseng and Fu, 2017a). In this section, we investigate the QBO influence on the thermodynamic properties of the TTL. Figure 4 shows the responses of zonal-mean temperature anomalies (T') and vertical temperature gradient anomalies (dT'/dz) to the QBO as a function of season, height, and lead of the QBO index.
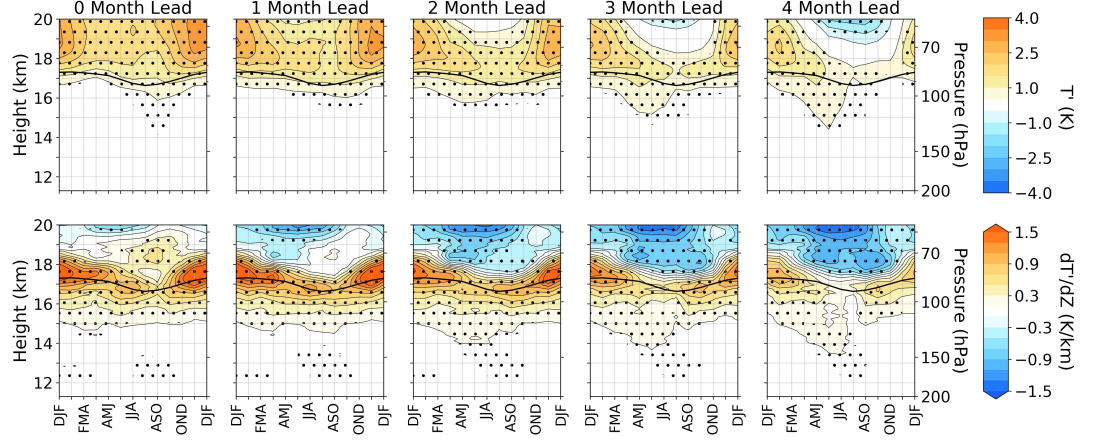
11

Figure 4: Seasonality of zonal-mean QBOW-QBOE anomaly composites averaged over 10°S-10°N as a function of height for temperature (row one) and vertical temperature gradients (row two). The columns, thick black lines, and stippling are the same as in Fig. 1.

Using a zero-month lead, T' shows a large seasonal variation in the QBOW-QBOE amplitude above ~18 km with peak magnitudes near 3.5 K in boreal winter. These results agree well with recent work showing that QBO-related lower-stratospheric and cold point tropopause (CPT) temperature changes tend to be largest in boreal winter (Tegtmeier et al., 2020; Sakeda et al., 2020; Hitchman et al., 2021; Martin et al., 2021a). The seasonality of QBO related T' above the tropopause matches that of vertical wind shear between 50 and 70 hPa (not shown). Although the QBO T' response is large above the tropopause, below the tropopause there is little impact in both zero- and one- month leads. However, using leads of two or more months reveals temperature intrusions which penetrate the troposphere reaching their maximum depth of 14.5 km. Importantly, this deep temperature intrusion is only evident during boreal spring and summer. The second row of Fig. 4 shows QBOW-QBOE composites in the vertical temperature gradient. Like the temperature intrusions observed in row one, the changes of vertical temperature gradient also exhibit deep tropospheric penetration with a seasonal preference of boreal spring and summer.

The frist row of Fig. 4 shows that zonal mean QBO temperature perturbations can penetrate to lower altitudes during boreal spring and summer when considering the QBO with a lead of 3-4 months. The seasonal cycle of vertical wind shear in the 70-150 hPa region was compared to that of T' below the tropopause. Unlike the T' above the tropopause, whose seasonality matches that of the vertical wind shear, below tropopause T' responses to the QBO do not share the same seasonality with vertical wind shear (not shown). This is likely because the seasonality of the QBO signal 70-150 hPa wind shear is too small to be

isolated from the larger variability associated with tropospheric processes. Regardless of why these T' responses penetrate into the troposphere, it remains to be explained why they only occur in boreal spring and summer.

Fundamentally, the QBO is characterized by changes in the zonal mean zonal wind. Figure 5 shows QBOW-QBOE composites of zonal-mean zonal wind anomalies (U') in the TTL region. It reveals a large U' response above 19 km that reaches amplitudes of greater than 15 m/s. Using a zero-month lead, the 20 km U' exhibits little seasonality. At greater leads, the 20 km U' seasonality grows in a way analogous to temperature anomalies shown in Fig. 4, as expected from the relation between temperatures and winds implied by thermal wind balance. From boreal spring to autumn the wind anomaly decays much faster with lead time than in boreal winter. In a modeling study, a similar faster decay of QBO jets near 50 hPa in boreal summer was attributed partially to the seasonal cycle of wave driving of the lower-stratospheric QBO jet and partially to the annual minimum in vertical velocity throughout the lower stratosphere during boreal summer (Krismer et al., 2013). When using leads of two to four months the zonal wind seasonality below the tropopause becomes more obvious. Deep intrusions of QBO-related zonal wind anomalies can reach as low as 15 km. Much like the anomalies seen for clouds (Fig. 1), temperature, and vertical temperature gradient (Fig. 4), these deep intrusions of zonal wind anomalies are only visible during boreal spring and summer (peak impact during MJJ). These zonal wind intrusions into the troposphere may be important for the general circulation of the upper troposphere, convective organization, and wave filtering of vertically propagating atmospheric waves (Baldwin et al., 2001; Collimore et al. 2003; Lane, 2021). Near 14 km and at leads of zero to two months a weak but statistically significant region of zonal wind anomalies opposite to those at higher levels is identified. A similar feature extending to lower levels has been found in other reanalysis data during boreal winter and spring (Gray et al., 2018; Hitchmann et al., 2020) and has been attributed to changes in the Walker circulation. This anomaly deserves more attention but is not further investigated here.
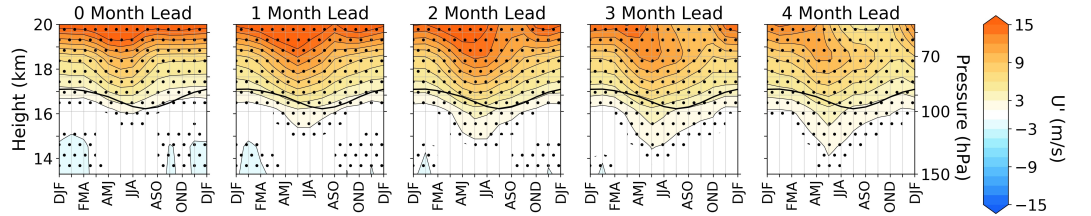

Figure 5: Seasonality of zonal-mean QBOW-QBOE anomaly composites averaged over 10°S-10°S as a function of height for zonal wind. The columns, thick black lines, and stippling are the same as in Fig. 1.

In summary, the observed seasonality in the tropical upper troposphere and TTL of the cloud fraction anomalies is synchronized with those of temperature,

vertical temperature gradient, and zonal wind: their deep intrusions all occur in boreal spring and early summer and maximize when the QBO index at 50 hPa leads by three months.

3.3 ERA5 zonal wind tendency analysis

Vertically extensive QBO-related signatures in cloud fraction are synchronized with tropospheric intrusions of QBO-related temperature and zonal wind (see Figs. 1, 4, and 5). In this section, we focus on the zonal wind signatures and attempt to document the physical processes that contribute to their creation and seasonality. For this zonal wind signature to travel downward into the TTL with time, there must be an acceleration of the zonal mean zonal winds. The idea that the seasonal cycle may impact QBO zonal wind accelerations is not new. It has long been known that the QBO jets near 50 hPa have seasonal variations in their accelerations, which has been linked to the preference of easterly QBO onsets at 50 hPa to occur during boreal spring and summer (Dunkerton and Delisi 1985; Dunkerton, 1990) and is manifested in the fastest descent of the QBO in these seasons (Wallace et al., 1993; Coy et al., 2020). It is possible that the upper tropospheric anomalies of zonal wind visible in Fig. 5 are at least indirectly tied to this seasonal preference of QBO acceleration and wind reversals.

To investigate the seasonal variations of lower-stratospheric zonal wind forcings and their potential impact on the tropospheric intrusions of zonal winds, we use the transformed eulerian mean (TEM) zonal mean zonal wind tendency equation (Andrews et al., 1987).

$$\frac{\partial \bar{u}}{\partial t} = \frac{1}{\rho_0 a\cos\phi}\nabla\cdot\mathbf{F} - \bar{w}^*\frac{\partial}{\partial z}(\bar{u}) - \frac{\bar{v}^*}{a\cos\phi}\frac{\partial(\bar{u}\cos\phi)}{\partial\phi} + f\bar{v}^* + \mathbf{X} \tag{1}$$

In Equation (1), overbars represent zonal averages and asterisks denote the TEM velocity. Variable f is the Coriolis parameter, a is the radius of the Earth, ϕ is the latitude, v is the meridional wind, w is the vertical velocity, ρ_0 is the density, $\nabla\cdot\mathbf{F}$ denotes the divergence of Eliassen-Palm (EP) flux vectors, and $\mathbf{X}$ denotes the unresolved tendencies (i.e., the necessary term which closes the budget at each timestep). The term on the left-hand side of the equation can be thought of as the net acceleration seen in ERA5. The terms on the right-hand side from left to right represent accelerations arising from the EP flux divergence (divergence of eddy heat and momentum fluxes), vertical advection, horizontal advection, Coriolis force, and the residual acceleration to close the budget.

Figure 6 shows the QBO-related signal for each of the terms in Eq. (1), calculated and displayed in the same way as for the anomalies previously shown in Figs. 1, 4 and 5, including for different lead times of the QBO winds at 50 hPa. Row one of Fig. 6 shows the QBO-related net zonal wind accelerations. At a zero-month lead, large accelerations peak around 70 hPa between late boreal winter and boreal summer, consistent with a relatively rapid descent of the QBO winds from 50 hPa in these seasons. With increasing lead time, these accelerations quickly disappear, and by a three-month lead almost all be-

come decelerations. These decelerations are associated with the reduction of the lower-stratospheric wind anomalies as seen in Fig. 5. Note that because the acceleration is the time derivative of zonal wind, its cumulative impact on the zonal wind is its integration over time. For example, if we are interested in the zonal wind anomalies in MJJ with a three-month lead of the QBO which penetrate into the troposphere reaching their peak, accelerations that will contribute to this impact and are observable in Fig. 6 will be those from FMA with a zero-month lead, MAM with a one-month lead, AMJ with a two-month lead, and MJJ with a three-month lead. The statistically significant zonal accelerations near 70 hPa and below at zero-, one-, and two-month leads near boreal spring may thus contribute to the below tropopause intrusions of zonal winds documented in this study.
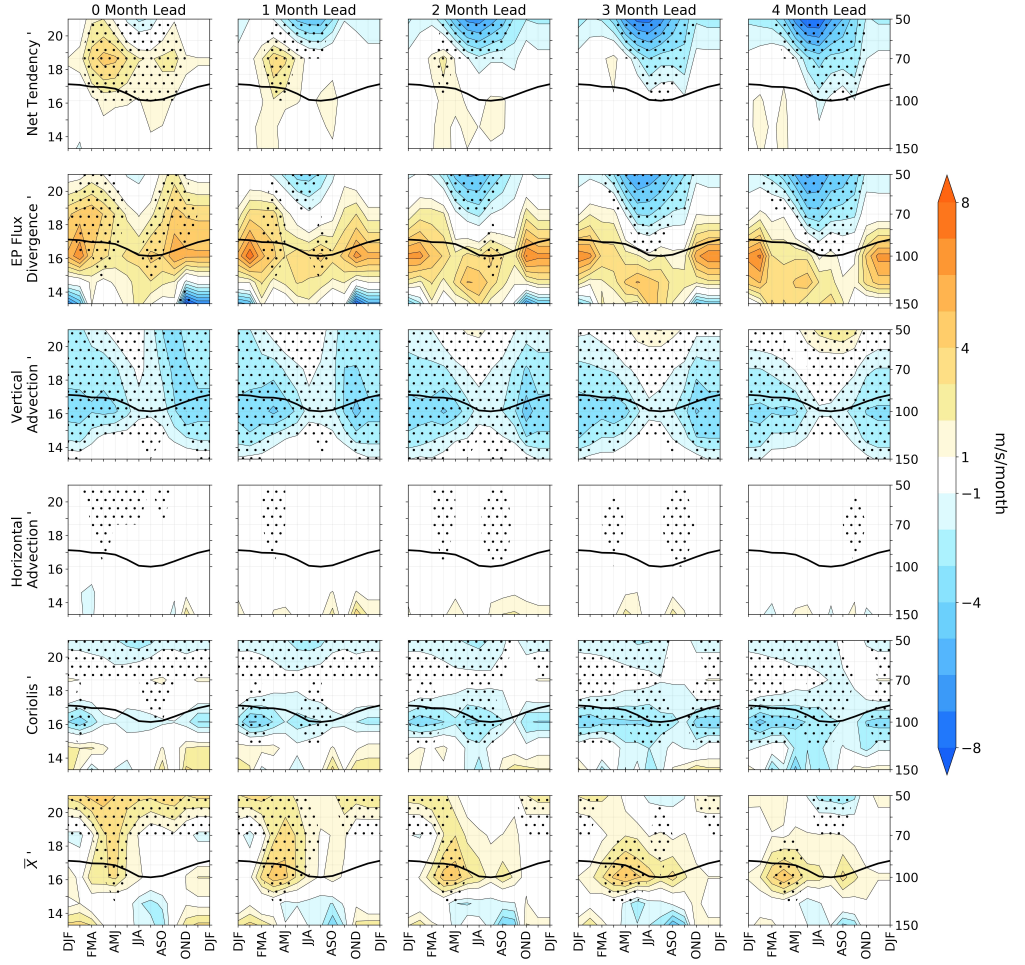
Figure 6: Seasonality of zonal-mean QBOW-QBOE accelerations averaged over 10°S-10°N as a function of height, for the net acceleration (row one), the EP flux divergence (row two), the vertical advection (row three), the horizontal advection (row four), the Coriolis force (row five) and the unresolved processes (row six). The columns, thick black lines, and stippling are the same as in Fig. 1.

We then look at the constituent components of the net acceleration on the right-

hand side of Eq. (1). The largest contribution to the net tendency comes from the EP flux divergence (row two of Fig. 6). Using a zero-month QBO lead, large accelerations due to the EP flux divergence are observed from ~16 to 20 km with a large seasonal variation. Pahlavan et al. (2021b) recently showed that a significant amount of the wave driving necessary for descent of the QBOW jet is resolved in the ERA5. Conversely, much of the easterly wind descent is tied to gravity waves that are only partly resolved in the ERA5 and would thus also show up in the residual acceleration. The EP flux divergence also contributes strongly to the breakdown of lower-stratospheric winds discussed above through the combined effects of Rossby, mixed Rossby-gravity, and Kelvin waves below about 20 km (see Fig. 10 in Pahlavan et al., 2021b). Other studies have noted seasonality in climatologies of Kelvin wave and Mixed Rossby-gravity wave activity in the TTL and lower stratosphere, with peak activity in boreal winter and spring (Maruyama, 1991; Tindall et al., 2006; Sjoberg et al., 2017).

The second largest component of the net tendency is the vertical advection (3rd row of Fig. 6). A strong seasonal cycle in this component is evident, which has its maximum near the tropopause in boreal winter and minimum in boreal summer. This is consistent with the known seasonal variation of the Brewer-Dobson circulation in the lower stratosphere (e.g., Rosenlof, 1995; Sevior et al., 2012). The vertical advection is related to the tropical upwelling, whereby increases in the tropical upwelling act to slow the downward propagation of the QBO (Wallace et al., 1993; Kinnersley and Pawson, 1996; Hampson and Haynes, 2004; Rajendran et al., 2018; Coy et al., 2020). Because of the similar seasonality and strong cancellation between the vertical advection and the EP flux divergence, it is difficult to determine the primary component setting the accelerations observed in the 1st row of Fig. 6.

The residual acceleration (6th row of Fig. 6) is contributed to by both unresolved gravity waves and model corrections required to nudge model predictions to observations. The peak acceleration in the net tendency at 70 hPa aligns well with those in the residual acceleration, suggesting that the unresolved processes in ERA5 are important in setting the seasonal cycle of the acceleration at 70 hPa. The residual acceleration peaks in AMJ, focused mainly above the tropopause with a zero-month QBO lead, but descends with increasing lead time. Below the tropopause, the residual acceleration is strongly damped by both the vertical advection and the Coriolis force (the same is true for the EP flux divergence). The least important process identified in the tendency analysis was the horizontal advection.

4 Discussion and Summary

This study documents the seasonality of the QBO impact on equatorial high clouds using 15 years of observations from the CALIPSO satellite. When using a QBO index based on zonal wind at the 50 hPa level with a three-month lead, significant cloud fraction responses extend down to 12 km, far below the region of strong QBO wind signal (>19 km). The magnitude of the QBO signal in zonal mean cloud fraction has a strong seasonal cycle, with deep intrusions only

occurring during boreal spring and summer. These deep cloud fraction changes culminate with a statistically significant and independently observed change in the longwave CRE. Synchronized with these vertically extensive cloud fraction changes, are QBO-related temperature and vertical temperature gradient changes that extended from above the tropopause to near 14 km. Measurements of these thermodynamic changes in the TTL came from GPS-RO data and are thus independent of the cloud data. QBO-related zonal winds from ERA5 were also shown to be synchronized with these cloud fraction and temperature changes. These results demonstrate a strong seasonality in the QBO signal in the TTL and tropical upper troposphere for the data period considered. These results are consistent with previous studies such as Collimore et al. (2003), Tegtmeier et al. (2020), Hitchman et al. (2021), and Martin et al. (2021a) but provide new evidence for the QBO signals in cloudiness and its vertical structure.

A remaining question regards the extent to which this seasonality is determined by the dynamics of the QBO within the lower stratosphere – a 'top-down' effect, or by the strong seasonality of the troposphere – a 'bottom-up' effect. Previous studies have suggested that the stratospheric QBO is influenced by the annual cycle through changes in the Semi-Annual Oscillation (Dunkerton, 1997; Kuai et al., 2009), the Brewer-Dobson Circulation (Hampson and Haynes, 2004; Rajendran et al., 2018; Coy et al., 2020), and the seasonality of wave-driving that reaches a given level of the atmosphere (Dunkerton, 1990; Maruyama, 1991). These would be 'top-down' effects. It may also be possible that the buffer zone (Match and Fueglistaler, 2019) which determines the lower limit of the QBO, undergoes a seasonal variation making the QBO signal in the upper troposphere larger in some seasons compared to others. If stratospheric processes set the seasonality of the tropospheric intrusions observed in this study, it may then represent an important component of stratospheric-tropospheric coupling. To analyze the potential importance of these processes in setting the seasonality of QBO impacts observed here, we used the TEM version of the zonal mean zonal wind tendency equation. We found evidence that the EP flux divergence, unresolved processes, and the vertical mean advection contribute to the seasonal cycle. This suggests that the seasonal cycles in wave-driving and the Brewer-Dobson Circulation are both important in setting the seasonal variations of QBO signals in the TTL. More research is needed regarding the extent to which stratospheric processes exert a "top-down" control on the observed seasonality of the QBO signal in the TTL.

Another potential mechanism by which the stratospheric QBO interacts with the tropical troposphere is through its effect on convection. In this mechanism, QBO-related temperature reductions in the upper TTL influence the CPT and static stability (Gray et al., 1992; Collimore et al., 2003; Davis et al., 2013; Nie and Sobel, 2015). Decreased TTL temperature and static stability associated with the QBOE allow for more vigorous and frequent deep convection which cools at altitudes near the TTL (Neelin and Holloway, 2007; Tegtmeier et al., 2020), creating an even more favorable environment for convection, and starting

a positive feedback loop. Similarly, increased temperatures associated with QBOW would decrease convection creating an analogous but opposite feedback. In this case, temperature and cloud fraction anomalies shown in Figs. 1 and 3 influence one another and propagate the QBO signal further into the troposphere and would represent a more "bottom-up" mechanism for the seasonality of the QBO signal in the TTL and upper troposphere. These feedbacks may be more effective in seasons when convection is more active.

This study also found a weak secondary minimum in zonal mean QBO-related TTL cirrus cloud fraction in DJF. This may be surprising given that the MJO, which strongly controls tropical high clouds (Virts et al., 2010; Son et al., 2017; Hendon and Abhik, 2018), was shown to have its strongest connection to the QBO in DJF. We find that much of the difference in the zonal mean cloud fraction signature between DJF and AMJ is due to longitudinal asymmetries in the cloud fraction response during DJF. Even though the zonal mean signature was weaker in DJF, TTL cirrus cloud field still shows strong responses in MJO active regions. Curiously, the AMJ cloud field also shows strong responses over MJO active regions yet there is little to no correlation between the MJO and QBO indices for this season (Son et al., 2017). In total, the DJF local minimum in zonal mean clouds should not be taken as evidence contrary to hypotheses linking the QBO and MJO through cirrus. Instead, results in this study lead to a separate question: If cirrus clouds are important to linking the QBO and MJO, why is there little connection during other seasons when the QBO related cirrus response is strong both in the zonal mean and over the MJO active longitudes?

In conclusion, this study shows that QBO-related changes in the equatorial high cloud fields can extend from tropopause to ~12 km and induce significant changes in the longwave CRE. These changes in cloud fraction are largely confined to boreal spring and summer and are synchronized with changes in temperature, vertical temperature gradient, and zonal wind in the TTL. Clouds and temperature are linked through convective and radiative effects, whereas temperature and zonal winds are linked through thermal wind balance, thus causal directions are difficult to decipher in this study. By noting that the data only span 15 years and thus only contain ~6 QBO cycles, longer data records will be required to confirm results of this study. However, this study does suggest that using the zonal mean equatorial region can provide perspective on the QBO direct impact on the troposphere. Critical to observing this connection is looking in boreal spring and summer when the connection is strongest. An important remaining question is what sets the seasonality of the QBO impact on the TTL.

Acknowledgments

Open Research

The code used to create this work is publicly available on Aodhan Sweeney's GitHub account.

References

Andrews, D. G., Holton, J. R., & Leovy, C. B. (1987). *Middle atmosphere dynamics*. https://www.osti.gov/biblio/5936274

Anstey, J. A., & Shepherd, T. G. (2014). High-latitude influence of the quasi-biennial oscillation. *Quarterly Journal of the Royal Meteorological Society*, *140*(678), 1–21. https://doi.org/10.1002/qj.2132

Baldwin, M. P., Gray, L. J., Dunkerton, T. J., Hamilton, K., Haynes, P. H., Randel, W. J., Holton, J. R., Alexander, M. J., Hirota, I., Horinouchi, T., Jones, D. B. A., Kinnersley, J. S., Marquardt, C., Sato, K., & Takahashi, M. (2001). The quasi-biennial oscillation. *Reviews of Geophysics*, *39*(2), 179–229. https://doi.org/10.1029/1999RG000073

Chang, K.-W., & L'Ecuyer, T. (2020). Influence of gravity wave temperature anomalies and their vertical gradients on cirrus clouds in the tropical tropopause layer – a satellite-based view. *Atmospheric Chemistry and Physics*, *20*(21), 12499–12514. https://doi.org/10.5194/acp-20-12499-2020

Collimore, C. C., Martin, D. W., Hitchman, M. H., Huesmann, A., & Waliser, D. E. (2003). On The Relationship between the QBO and Tropical Deep Convection. *Journal of Climate*, *16*(15), 2552–2568. https://doi.org/10.1175/1520-0442(2003)016<2552:OTRBTQ>2.0.CO;2

Corti, T., Luo, B. P., Fu, Q., Vömel, H., & Peter, T. (2006). The impact of cirrus clouds on tropical troposphere-to-stratosphere transport. *Atmospheric Chemistry and Physics*, *6*(9), 2539–2547. https://doi.org/10.5194/acp-6-2539-2006

Corti, T., Luo, B. P., Peter, T., Vömel, H., & Fu, Q. (2005). Mean radiative energy balance and vertical mass fluxes in the equatorial upper troposphere and lower stratosphere. *Geophysical Research Letters*, *32*(6). https://doi.org/10.1029/2004GL021889

Coy, L., Newman, P. A., Strahan, S., & Pawson, S. (2020). Seasonal Variation of the Quasi-Biennial Oscillation Descent. *Journal of Geophysical Research: Atmospheres*, *125*(18), e2020JD033077. https://doi.org/10.1029/2020JD033077

Davis, S. M., Liang, C. K., & Rosenlof, K. H. (2013). Interannual variability of tropical tropopause layer clouds. *Geophysical Research Letters*, *40*(11), 2862–2866. https://doi.org/10.1002/grl.50512

Densmore, C. R., Sanabia, E. R., & Barrett, B. S. (2019). QBO Influence on MJO Amplitude over the Maritime Continent: Physical Mechanisms and Seasonality. *Monthly Weather Review*, *147*(1), 389–406. https://doi.org/10.1175/MWR-D-18-0158.1

Dessler, A. E., Schoeberl, M. R., Wang, T., Davis, S. M., & Rosenlof, K. H. (2013). Stratospheric water vapor feedback. *Proceedings of the National Academy of Sciences*, *110*(45), 18087–18091. https://doi.org/10.1073/pnas.1310344110

Ding, Q., & Fu, Q. (2018). A warming tropical central Pacific dries the lower stratosphere. *Climate Dynamics*, *50*(7), 2813–2827. https://doi.org/10.1007/s00382-017-3774-y

Dunkerton, T. (1990). *Annual variation of deseasonalized mean flow acceleration in the equatorial lower stratosphere.* https://doi.org/10.2151/JMSJ1965.68.4_499

Dunkerton, T. J. (1997). The role of gravity waves in the quasi-biennial oscillation. *Journal of Geophysical Research: Atmospheres*, *102*(D22), 26053–26076. https://doi.org/10.1029/96JD02999

Dunkerton, T. J., & Delisi, D. P. (1985). Climatology of the Equatorial Lower Stratosphere. *Journal of the Atmospheric Sciences*, *42*(4), 376–396. https://doi.org/10.1175/1520-0469(1985)042<0376:COTELS>2.0.CO;2

Flury, T., Wu, D. L., & Read, W. G. (2012). Correlation among cirrus ice content, water vapor and temperature in the TTL as observed by CALIPSO and Aura/MLS. *Atmospheric Chemistry and Physics*, *12*(2), 683–691. https://doi.org/10.5194/acp-12-683-2012

Fu, Q., Hu, Y., & Yang, Q. (2007). Identifying the top of the tropical tropopause layer from vertical mass flux analysis and CALIPSO lidar cloud observations. *Geophysical Research Letters*, *34*(14). https://doi.org/10.1029/2007GL030099

Fu, Q., Smith, M., & Yang, Q. (2018). The Impact of Cloud Radiative Effects on the Tropical Tropopause Layer Temperatures. *Atmosphere*, *9*(10), 377. https://doi.org/10.3390/atmos9100377

Fueglistaler, S., Dessler, A. E., Dunkerton, T. J., Folkins, I., Fu, Q., & Mote, P. W. (2009). Tropical tropopause layer. *Reviews of Geophysics*, *47*(1). https://doi.org/10.1029/2008RG000267

Fueglistaler, S., & Haynes, P. H. (2005). Control of interannual and longer-term variability of stratospheric water vapor. *Journal of Geophysical Research: Atmospheres*, *110*(D24). https://doi.org/10.1029/2005JD006019

Gabis, I. P. (2018). Seasonal dependence of the quasi-biennial oscillation (QBO): New evidence from IGRA data. *Journal of Atmospheric and Solar-Terrestrial Physics*, *179*, 316–336. https://doi.org/10.1016/j.jastp.2018.08.012

Giorgetta, M. A., Bengtsson, L., & Arpe, K. (1999). An investigation of QBO signals in the east Asian and Indian monsoon in GCM experiments. *Climate Dynamics*, *15*(6), 435–450. https://doi.org/10.1007/s003820050292

Gray, L. J., Anstey, J. A., Kawatani, Y., Lu, H., Osprey, S., & Schenzinger, V. (2018). Surface impacts of the Quasi Biennial Oscillation. *Atmospheric Chemistry and Physics*, *18*(11), 8227–8247. https://doi.org/10.5194/acp-18-8227-2018

Gray, W. M., Sheaffer, J. D., & Knaff, J. A. (1992). Influence of the Stratospheric QBO on ENSO Variability. *Journal of the Meteorological Society of Japan. Ser. II*, *70*(5), 975–995. https://doi.org/10.2151/jmsj1965.70.5_975

Hampson, J., & Haynes, P. (2004). Phase Alignment of the Tropical Stratospheric QBO in the Annual Cycle. *Journal of the Atmospheric Sciences*, *61*(21), 2627–2637. https://doi.org/10.1175/JAS3276.1

Hartmann, D. L., Holton, J. R., & Fu, Q. (2001). The heat balance of the tropical tropopause, cirrus, and stratospheric dehydration. *Geophysical Research Letters*, *28*(10), 1969–1972. https://doi.org/10.1029/2000GL012833

Haynes, P., Hitchcock, P., Hitchman, M., Yoden, S., Hendon, H., Kiladis, G., Kodera, K., & Simpson, I. (2021). The Influence of the Stratosphere on the Tropical Troposphere. *Journal of the Meteorological Society of Japan. Ser. II*, *99*(4), 803–845. https://doi.org/10.2151/jmsj.2021-040

Hendon, H. H., & Abhik, S. (2018). Differences in Vertical Structure of the Madden-Julian Oscillation Associated With the Quasi-Biennial Oscillation. *Geophysical Research Letters*, *45*(9), 4419–4428. https://doi.org/10.1029/2018GL077207

Hitchman, M. H., Yoden, S., Haynes, P. H., Kumar, V., & Tegtmeier, S. (2021). An Observational History of the Direct Influence of the Stratospheric Quasi-biennial Oscillation on the Tropical and Subtropical Upper Troposphere and Lower Stratosphere. *Journal of the Meteorological Society of Japan. Ser. II*, *99*(2), 239–267. https://doi.org/10.2151/jmsj.2021-012

Holloway, C. E., & Neelin, J. D. (2007). The Convective Cold Top and Quasi Equilibrium. *Journal of the Atmospheric Sciences*, *64*(5), 1467–1487. https://doi.org/10.1175/JAS3907.1

Holton, J. R., & Lindzen, R. S. (1972). An Updated Theory for the Quasi-Biennial Cycle of the Tropical Stratosphere. *Journal of the Atmospheric Sciences*, *29*(6), 1076–1080. https://doi.org/10.1175/1520-0469(1972)029<1076:AUTFTQ>2.0.CO;2

Holton, J. R., & Tan, H.-C. (1980). The Influence of the Equatorial Quasi-Biennial Oscillation on the Global Circulation at 50 mb. *Journal of the Atmospheric Sciences*, *37*(10), 2200–2208. https://doi.org/10.1175/1520-0469(1980)037<2200:TIOTEQ>2.0.CO;2

Holton, J. R., & Tan, H.-C. (1982). The Quasi-Biennial Oscillation in the Northern Hemisphere Lower Stratosphere. *Journal of the Meteorological Society of Japan. Ser. II*, *60*(1), 140–148. https://doi.org/10.2151/jmsj1965.60.1_140

Hong, Y., Liu, G., & Li, J.-L. F. (2016). Assessing the Radiative Effects of Global Ice Clouds Based on CloudSat and CALIPSO Measurements. *Journal of Climate*, *29*(21), 7651–7674. https://doi.org/10.1175/JCLI-D-15-0799.1

Huesmann, A. S., & Hitchman, M. H. (2001). The stratospheric quasi-biennial oscillation in the NCEP reanalyses: Climatological structures. *Journal of Geophysical Research: Atmospheres*, *106*(D11), 11859–11874. https://doi.org/10.1029/2001JD900031

Kim, J.-E., Alexander, M. J., Bui, T. P., Dean-Day, J. M., Lawson, R. P., Woods, S., Hlavka, D., Pfister, L., & Jensen, E. J. (2016). Ubiquitous influence of waves on tropical high cirrus clouds. *Geophysical Research Letters*, *43*(11), 5895–5901. https://doi.org/10.1002/2016GL069293

Kinnersley, J. S., & Pawson, S. (1996). The Descent Rates of the Shear Zones of the Equatorial QBO. *Journal of the Atmospheric Sciences*, *53*(14), 1937–1949. https://doi.org/10.1175/1520-0469(1996)053<1937:TDROTS>2.0.CO;2

Klotzbach, P., Abhik, S., Hendon, H. H., Bell, M., Lucas, C., G. Marshall, A., & Oliver, E. C. J. (2019). On the emerging relationship between the stratospheric Quasi-Biennial oscillation and the Madden-Julian oscillation. *Scientific Reports*, *9*(1), 2981. https://doi.org/10.1038/s41598-019-40034-6

Krismer, T. R., Giorgetta, M. A., & Esch, M. (2013). Seasonal aspects of the quasi-biennial oscillation in the Max Planck Institute Earth System Model and ERA-40. *Journal of Advances in Modeling Earth Systems*, *5*(2), 406–421. https://doi.org/10.1002/jame.20024

Kuai, L., Shia, R.-L., Jiang, X., Tung, K.-K., & Yung, Y. L. (2009). Non-stationary Synchronization of Equatorial QBO with SAO in Observations and a Model. *Journal of the Atmospheric Sciences*, *66*(6), 1654–1664. https://doi.org/10.1175/2008JAS2857.1

Kuo, Y.-H., Wee, T.-K., Sokolovskiy, S., Rocken, C., Schreiner, W., Hunt, D., & Anthes, R. A. (2004). Inversion and Error Estimation of GPS Radio Occultation Data. *Journal of the Meteorological Society of Japan. Ser. II*, *82*(1B), 507–531. https://doi.org/10.2151/jmsj.2004.507

Kursinski, E. R., Hajj, G. A., Schofield, J. T., Linfield, R. P., & Hardy, K. R. (1997). Observing Earth's atmosphere with radio occultation measurements using the Global Positioning System. *Journal of Geophysical Research: Atmospheres*, *102*(D19), 23429–23465. https://doi.org/10.1029/97JD01569

Lane, T. P. (2021). Does Lower-Stratospheric Shear Influence the Mesoscale Organization of Convection? *Geophysical Research Letters*, *48*(3), e2020GL091025. https://doi.org/10.1029/2020GL091025

Liess, S., & Geller, M. A. (2012). On the relationship between QBO and distribution of tropical deep convection. *Journal of Geophysical Research: Atmospheres*, *117*(D3). https://doi.org/10.1029/2011JD016317

Lin, J., & Emanuel, K. (2022). *Stratospheric Modulation of the MJO through Cirrus Cloud Feedbacks*. https://doi.org/10.48550/arXiv.2204.02379

Lindzen, R. S., & Holton, J. R. (1968). A Theory of the Quasi-Biennial Oscillation. *Journal of the Atmospheric Sciences*, *25*(6), 1095–1107. https://doi.org/10.1175/1520-0469(1968)025<1095:ATOTQB>2.0.CO;2

Loeb, N. G., Doelling, D. R., Wang, H., Su, W., Nguyen, C., Corbett, J. G., Liang, L., Mitrescu, C., Rose, F. G., & Kato, S. (2018). Clouds and the Earth's

Radiant Energy System (CERES) Energy Balanced and Filled (EBAF) Top-of-Atmosphere (TOA) Edition-4.0 Data Product. *Journal of Climate*, *31*(2), 895–918. https://doi.org/10.1175/JCLI-D-17-0208.1

Lu, H., Hitchman, M. H., Gray, L. J., Anstey, J. A., & Osprey, S. M. (2020). On the role of Rossby wave breaking in the quasi-biennial modulation of the stratospheric polar vortex during boreal winter. *Quarterly Journal of the Royal Meteorological Society*, *146*(729), 1939–1959. https://doi.org/10.1002/qj.3775

Martin, Z., Sobel, A., Butler, A., & Wang, S. (2021). Variability in QBO Temperature Anomalies on Annual and Decadal Time Scales. *Journal of Climate*, *34*(2), 589–605. https://doi.org/10.1175/JCLI-D-20-0287.1

Martin, Z., Son, S.-W., Butler, A., Hendon, H., Kim, H., Sobel, A., Yoden, S., & Zhang, C. (2021). The influence of the quasi-biennial oscillation on the Madden–Julian oscillation. *Nature Reviews Earth & Environment*, *2*(7), 477–489. https://doi.org/10.1038/s43017-021-00173-9

Martin, Z., Wang, S., Nie, J., & Sobel, A. (2019). The Impact of the QBO on MJO Convection in Cloud-Resolving Simulations. *Journal of the Atmospheric Sciences*, *76*(3), 669–688. https://doi.org/10.1175/JAS-D-18-0179.1

Maruyama, T. (1991). Annual and QBO-Synchronized Variations of Lower-Stratospheric Equatorial Wave Activity over Singapore during 1961-1989. *Journal of the Meteorological Society of Japan. Ser. II*, *69*(2), 219–232. https://doi.org/10.2151/jmsj1965.69.2_219

Match, A., & Fueglistaler, S. (2019). The Buffer Zone of the Quasi-Biennial Oscillation. *Journal of the Atmospheric Sciences*, *76*(11), 3553–3567. https://doi.org/10.1175/JAS-D-19-0151.1

Mote, P. W., Rosenlof, K. H., McIntyre, M. E., Carr, E. S., Gille, J. C., Holton, J. R., Kinnersley, J. S., Pumphrey, H. C., Russell III, J. M., & Waters, J. W. (1996). An atmospheric tape recorder: The imprint of tropical tropopause temperatures on stratospheric water vapor. *Journal of Geophysical Research: Atmospheres*, *101*(D2), 3989–4006. https://doi.org/10.1029/95JD03422

Murayama, Y., Tsuda, T., & Fukao, S. (1994). Seasonal variation of gravity wave activity in the lower atmosphere observed with the MU radar. *Journal of Geophysical Research: Atmospheres*, *99*(D11), 23057–23069. https://doi.org/10.1029/94JD01717

Nie, J., & Sobel, A. H. (2015). Responses of Tropical Deep Convection to the QBO: Cloud-Resolving Simulations. *Journal of the Atmospheric Sciences*, *72*(9), 3625–3638. https://doi.org/10.1175/JAS-D-15-0035.1

Pahlavan, H. A., Fu, Q., Wallace, J. M., & Kiladis, G. N. (2021). Revisiting the Quasi-Biennial Oscillation as Seen in ERA5. Part I: Description and Momentum Budget. *Journal of the Atmospheric Sciences*, *78*(3), 673–691. https://doi.org/10.1175/JAS-D-20-0248.1

Pahlavan, H. A., Wallace, J. M., Fu, Q., & Kiladis, G. N. (2021). Revisiting the Quasi-Biennial Oscillation as Seen in ERA5. Part II: Evaluation of Waves and Wave Forcing. *Journal of the Atmospheric Sciences*, *78*(3), 693–707. https://doi.org/10.1175/JAS-D-20-0249.1

Plumb, R. A., & Bell, R. C. (1982). A model of the quasi-biennial oscillation on an equatorial beta-plane. *Quarterly Journal of the Royal Meteorological Society*, *108*(456), 335–352. https://doi.org/10.1002/qj.49710845604

Rajendran, K., Moroz, I. M., Osprey, S. M., & Read, P. L. (2018). Descent Rate Models of the Synchronization of the Quasi-Biennial Oscillation by the Annual Cycle in Tropical Upwelling. *Journal of the Atmospheric Sciences*, *75*(7), 2281–2297. https://doi.org/10.1175/JAS-D-17-0267.1

Rosenlof, K. H. (1995). Seasonal cycle of the residual mean meridional circulation in the stratosphere. *Journal of Geophysical Research: Atmospheres*, *100*(D3), 5173–5191. https://doi.org/10.1029/94JD03122

Sakaeda, N., Dias, J., & Kiladis, G. N. (2020). The Unique Characteristics and Potential Mechanisms of the MJO-QBO Relationship. *Journal of Geophysical Research: Atmospheres*, *125*(17), e2020JD033196. https://doi.org/10.1029/2020JD033196

Saravanan, R. (1990). A Multiwave Model of the Quasi-biennial Oscillation. *Journal of the Atmospheric Sciences*, *47*(21), 2465–2474. https://doi.org/10.1175/1520-0469(1990)047<2465:AMMOTQ>2.0.CO;2

Sjoberg, J. P., Birner, T., & Johnson, R. H. (2017). Intraseasonal to interannual variability of Kelvin wave momentum fluxes as derived from high-resolution radiosonde data. *Atmospheric Chemistry and Physics*, *17*(14), 8971–8986. https://doi.org/10.5194/acp-17-8971-2017

Sokol, A. B., & Hartmann, D. L. (2020). Tropical Anvil Clouds: Radiative Driving Toward a Preferred State. *Journal of Geophysical Research: Atmospheres*, *125*(21), e2020JD033107. https://doi.org/10.1029/2020JD033107

Son, S.-W., Lim, Y., Yoo, C., Hendon, H. H., & Kim, J. (2017). Stratospheric Control of the Madden–Julian Oscillation. *Journal of Climate*, *30*(6), 1909–1922. https://doi.org/10.1175/JCLI-D-16-0620.1

Tegtmeier, S., Anstey, J., Davis, S., Ivanciu, I., Jia, Y., McPhee, D., & Pilch Kedzierski, R. (2020). Zonal Asymmetry of the QBO Temperature Signal in the Tropical Tropopause Region. *Geophysical Research Letters*, *47*(24), e2020GL089533. https://doi.org/10.1029/2020GL089533

Tian, E. W., Su, H., Tian, B., & Jiang, J. H. (2019). Interannual variations of water vapor in the tropical upper troposphere and the lower and middle stratosphere and their connections to ENSO and QBO. *Atmospheric Chemistry and Physics*, *19*(15), 9913–9926. https://doi.org/10.5194/acp-19-9913-2019

Tindall, J. C., Thuburn, J., & Highwood, E. J. (2006). Equatorial waves

in the lower stratosphere. II: Annual and interannual variability. *Quarterly Journal of the Royal Meteorological Society*, *132*(614), 195–212. https://doi.org/10.1256/qj.04.153

Tseng, H.-H., & Fu, Q. (2017a). Temperature Control of the Variability of Tropical Tropopause Layer Cirrus Clouds. *Journal of Geophysical Research: Atmospheres*, *122*(20), 11,062-11,075. https://doi.org/10.1002/2017JD027093

Tseng, H.-H., & Fu, Q. (2017b). Tropical tropopause layer cirrus and its relation to tropopause. *Journal of Quantitative Spectroscopy and Radiative Transfer*, *188*, 118–131. https://doi.org/10.1016/j.jqsrt.2016.05.029

Virts, K. S., & Wallace, J. M. (2014). Observations of Temperature, Wind, Cirrus, and Trace Gases in the Tropical Tropopause Transition Layer during the MJO. *Journal of the Atmospheric Sciences*, *71*(3), 1143–1157. https://doi.org/10.1175/JAS-D-13-0178.1

Virts, K. S., Wallace, J. M., Fu, Q., & Ackerman, T. P. (2010). Tropical Tropopause Transition Layer Cirrus as Represented by CALIPSO Lidar Observations. *Journal of the Atmospheric Sciences*, *67*(10), 3113–3129. https://doi.org/10.1175/2010JAS3412.1

Wallace, J. M., Panetta, R. L., & Estberg, J. (1993). Representation of the Equatorial Stratospheric Quasi-Biennial Oscillation in EOF Phase Space. *Journal of the Atmospheric Sciences*, *50*(12), 1751–1762. https://doi.org/10.1175/1520-0469(1993)050<1751:ROTESQ>2.0.CO;2

Wang, M., & Fu, Q. (2021). Stratosphere-Troposphere Exchange of Air Masses and Ozone Concentrations Based on Reanalyses and Observations. *Journal of Geophysical Research: Atmospheres*, *126*(18), e2021JD035159. https://doi.org/10.1029/2021JD035159

Winker, D. M., Pelon, J., Coakley, J. A., Ackerman, S. A., Charlson, R. J., Colarco, P. R., Flamant, P., Fu, Q., Hoff, R. M., Kittaka, C., Kubar, T. L., Treut, H. L., Mccormick, M. P., Mégie, G., Poole, L., Powell, K., Trepte, C., Vaughan, M. A., & Wielicki, B. A. (2010). The CALIPSO Mission: A Global 3D View of Aerosols and Clouds. *Bulletin of the American Meteorological Society*, *91*(9), 1211–1230. https://doi.org/10.1175/2010BAMS3009.1

Yamazaki, K., Nakamura, T., Ukita, J., & Hoshi, K. (2020). A tropospheric pathway of the stratospheric quasi-biennial oscillation (QBO) impact on the boreal winter polar vortex. *Atmospheric Chemistry and Physics*, *20*(8), 5111–5127. https://doi.org/10.5194/acp-20-5111-2020

Yang, Q., Fu, Q., & Hu, Y. (2010). Radiative impacts of clouds in the tropical tropopause layer. *Journal of Geophysical Research: Atmospheres*, *115*(D4). https://doi.org/10.1029/2009JD012393

Yoo, C., & Son, S.-W. (2016). Modulation of the boreal wintertime Madden-Julian oscillation by the stratospheric quasi-biennial oscillation. *Geophysical Research Letters*, *43*(3), 1392–1398. https://doi.org/10.1002/2016GL067762

Zeng, Z., Sokolovskiy, S., Schreiner, W. S., & Hunt, D. (2019). Representation of Vertical Atmospheric Structures by Radio Occultation Observations in the Upper Troposphere and Lower Stratosphere: Comparison to High-Resolution Radiosonde Profiles. *Journal of Atmospheric and Oceanic Technology*, *36*(4), 655–670. https://doi.org/10.1175/JTECH-D-18-0105.1